Probing the Effect of Salt on Asphaltene Aggregation in Aqueous Solutions Using Molecular Dynamics Simulations

Journal:	*Energy & Fuels*
Manuscript ID	ef-2018-01191v.R1
Manuscript Type:	Article
Date Submitted by the Author:	29-May-2018
Complete List of Authors:	Sun, Xiaoyu; University of Alberta, Chemical and Materials Engineering Jian, Cuiying; University of Alberta, Chemical and Material Engineering & Mechanical Engineering He, Yingkai; University of Alberta, Mechanical Engineering Zeng, Hongbo; University of Alberta, Chemical and Materials Engineering Tang, Tian; University of Alberta, Mechanical Engineering

Probing the Effect of Salt on Asphaltene Aggregation in Aqueous Solutions Using Molecular Dynamics Simulations

Xiaoyu Sun[†], Cuiying Jian[‡], Yingkai He[‡], Hongbo Zeng[,†], Tian Tang[*,‡]*

[†]Department of Chemical and Materials Engineering, University of Alberta, Edmonton, AB T6G 2V4, Canada

[‡]Department of Mechanical Engineering, University of Alberta, Edmonton, AB T6G 2V4, Canada

** Corresponding author:*

E-mail: hongbo.zeng@ualberta.ca (H.Z.); Phone: +1-780-492-1044;

E-mail: tian.tang@ualberta.ca (T.T.); Phone: +1-780-492-5467.

ABSTRACT

The presence of salts in different processes of oil production has attracted wide attention because of its effects on asphaltene aggregation, stability and interactions of emulsions, etc. In this work, molecular dynamics simulations were employed to study the effect of salts on aggregation of model asphaltenes. Four types of polyaromatic compounds possessing key structural features of continental-type asphaltenes were dispersed into NaCl solutions of different concentrations. These models have the same polyaromatic core but different lengths for the side chains. In the two models with relatively long side chains, the hydrophobic association among side chains is the main driving force for aggregation. The effect of salt on aggregation is therefore closely tied to its influence on the hydrophobic interaction: the salt ions promote the hydrophobic interaction at low salt concentration while suppressing it at high salt concentration. For the model with intermediate side chain length, the hydrophobic interaction between side chains becomes less dominant, and the salt has mutual influences on the core-core, chain-chain and core-chain interactions. For the model with the shortest side chains, although the core-core and core-chain interactions are more important, the side chains still play a role in aggregation when the salt is present. Our results provide new insights into the fundamental understanding of the influence of salts on the aggregation and interaction behaviors of polyaromatic compounds in aqueous environment.

1. INTRODUCTION

Asphaltenes are the heaviest components in crude oil.[1] Their aggregation and interfacial activities pose serious problems during oil production, such as changing the wettability of oil reservoir, choking the pore throats, and stabilizing the interface between water and oil.[2,3,12,4–11] Spontaneous aggregation of asphaltenes is mostly studied in toluene, in which asphaltenes are by definition soluble. It was observed that above the critical nanoaggregate concentration (CNAC), on the order of 100 mg/L, nanoaggregates are formed each containing a small number of molecules (<10). At higher concentrations (several g/L), the nanoaggregate can associate into clusters.[13,14] The clusters have various sizes, as small as 6 nm and up to tens of nanometers or more.[15]

The most well-known model that describes the aggregation behavior of asphaltenes is the Yen-Mullins model,[14,16] which considers the continental-type asphaltene that consists of a polycyclic aromatic (PA) core attached with peripheral hydrocarbon chains.[17,18] Supported by many experiments,[13,19] the nanoaggregate in the Yen-Mullins model has a stack of PA cores surrounded by aliphatic side chains. The aggregation is mostly attributed to the π–π interaction between the PA cores, while the side chains exhibit steric repulsion in toluene and hinder the association of PA cores.[20,21] In aqueous solutions, however, the hydrophobic association between side chains becomes another driving force for asphaltene aggregation.[21,22] In the molecular dynamics (MD) simulations by Jian et al.,[21] hydrophobic interaction contributed significantly to the aggregation of model compounds with long side chains. By reducing the length of the side chains, the size of the aggregates decreased due to the reduced degree of side chain association. Only when the side chains were sufficiently small the aggregation could be enhanced again due to the diminishing interference of the side chains with the π-π interaction. The mechanisms of

aggregation are therefore largely dependent on the structures of asphaltene molecules and the nature of the solvents.

Salt is another factor that can influence the behaviors of asphaltenes, since water or brine water is widely applied in water-flooding during the recovery process.[23–25] In carbonate reservoirs, the salt in water can reach a concentration as high as 250 000 ppm,[26] which impacts the viscosity of crude oil, interfacial tension between water and oil, and wettability of oil reservoirs.[27] It is therefore important to understand the role of salinity during the oil production processes. Rezaeidoust et al. discovered that the solubility of asphaltene in low salinity water was significantly decreased by increasing salt concentration,[25,28] which could in turn promote the aggregate of asphaltene molecules. They attributed the observation to the salting-out effect, viz., the cations (Na^+, Ca^{2+}) interfered with the water structure around the organic molecules, thus decreasing their solubility. Chaala et al. also found that salt deposits in flooding water promoted the flocculation of asphaltenes.[29] Liu et al.[30] and Zhang, et al.[31] measured the interfacial forces between asphaltene films in aqueous solutions by an atomic force microscope (AFM) and surface forces apparatus (SFA), respectively. The results suggested that the adhesion force between asphaltene films was slightly increased upon the addition of 100 mM KCl[30] or 100 mM NaCl, which was more significantly enhanced upon the addition of 1-100 mM $CaCl_2$[31]. Previous studies also investigated the effect of salt on the behaviors of asphaltenes adsorbed on water/oil interfaces, since the accumulation of asphaltenes on the interfaces tends to cause a reduction in the interfacial tension (IFT).[32] In the presence of low salinity water, asphaltene accumulation on the water/oil interface is prominent, and several independent works reported a reduction of IFT.[11,23,33–35] When the salt concentration is sufficiently high (~40,000 ppm), Moeini et al. observed that the IFT started to increase with further addition of salt. This reversed trend was

attributed to the salting-out effect, which decreased the solubility of asphaltene in water, increased its solubility in oil, and reduced asphaltene accumulation on the interface.[34]

Despite the above experimental work, mechanistic understanding on the effect of salinity on asphaltene aggregation is not yet completely clear, especially at the molecular level. Such effect is likely dependent on the molecular structure of the asphaltenes, which has not been investigated. Motivated by these, we performed a series of MD simulations to study the aggregation of model asphaltene compounds in water with the presence of salt (NaCl). Below the saturation concentration of NaCl (26% wt. at 20°C), we selected three different concentrations (5% wt., 10% wt. and 15% wt.), in addition to the case of pure water (no salt). Variations in the molecular structures of the model compounds were also studied. This work provides new insights into how salinity impacts the asphaltene aggregation and the interplay between salinity and different moieties (PA core, side chains) on the asphaltenes.

2. SIMULATION METHODS

2.1 Molecular models.

The model asphaltene compounds simulated in this work are based on Violantrone-78 ($C_{70}H_{84}O_6$, VO-78),[36] shown in Figure 1a. It has the typical structure and properties of continental-type asphaltene, containing a polyaromatic core and aliphatic side chains, and has been employed widely as a model compound to study the aggregation behaviour of asphaltenes.[12,21,22,37–40] In order to investigate the effect of molecular structure, three models were constructed in addition to the original VO-78, by varying the side chain length. These models are shown in Figures 1b to 1d, where the number of carbon atoms in each side chain attached to –

COO- is reduced from 16 in VO-78 to 12, 8 and 4, respectively. The four models will be denoted as VO-16C, VO-12C, VO-8C and VO-4C in this work.

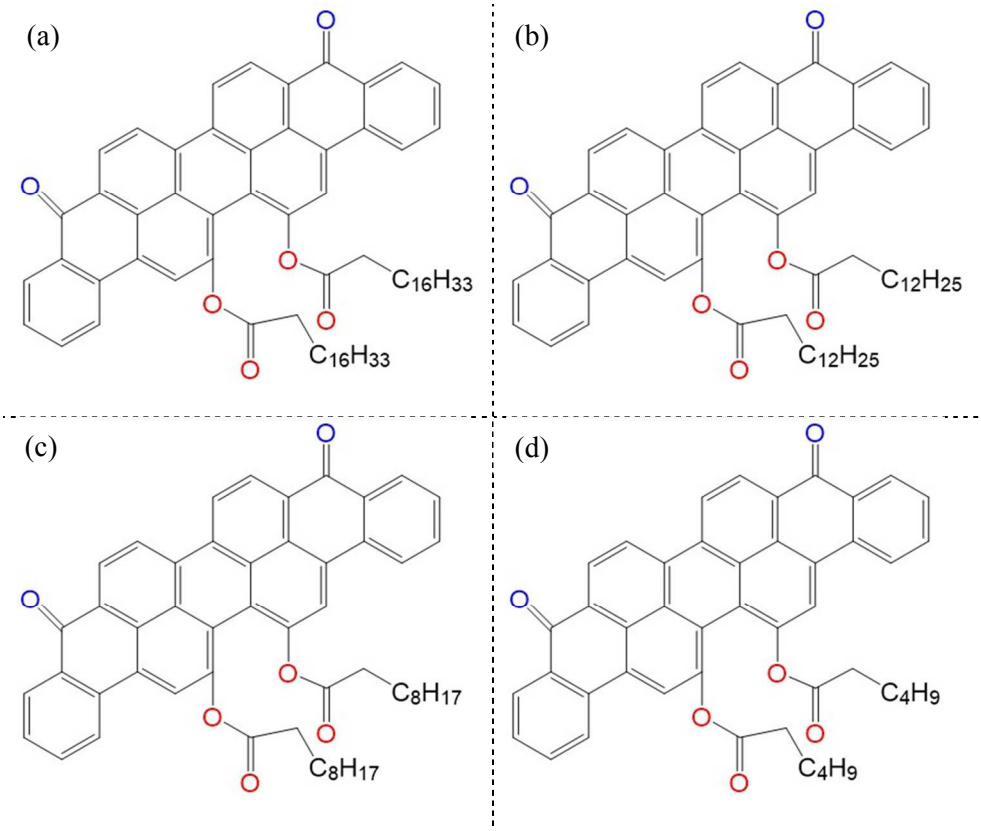

Figure 1. Molecular structures of (a) VO-16C, (b) VO-12C, (c) VO-8C and (d) VO-4C. The 2 oxygen atoms bonded to the core are colored blue, and the 4 oxygen atoms on the side chains are colored red.

The molecular structure of VO-16C was generated using the Chem3D Ultra 10.0 software. By manually adjusting the number of carbon atoms on the side chains, the structures of VO-12C, VO-8C and VO-4C were obtained. The coordinate files of each model were submitted to GlycoBioChem PRODRG2 server,[41] which generated the corresponding topology files. The partial charges and charge groups in the topology were manually modified in order to be compatible with the force field GROMOS96 53A6[42]. Supporting Information Section S1 shows

the partial atomic charges of the model compounds, which were proposed and validated in our previous studies[21,22,39,40,43].

2.2 Simulation details.

In each simulation, 24 molecules of a particular type of model compound were introduced into a cubic box with side length of 12 nm in the form of a 2 × 3 × 4 array. The box was large enough to ensure all solute molecules were at least 1.8 nm from the edge of the box. The box was then filled with simple-point-charge (SPC) water, which has been proven suitable to simulate the interaction between water and asphaltene molecules.[44–46] The concentration of asphaltenes was around 20 g/L so nanoaggregates were expected to be formed.

To investigate the effect of salinity, different amount of NaCl was added to the water box to reach salt concentrations of 5% wt. 10% wt. and 15% wt. respectively. All systems simulated in this work are listed in Table 1, where each system is named by the concentration of NaCl and the type of asphaltene models. For example, 5%-4C represents the system with 24 VO-4C molecules in 5% wt. NaCl solution.

Table 1. Details of the simulated systems.

System	NaCl concentration (mM)	Model compounds
5%-16C	854.5	VO-16C
5%-12C	856.3	VO-12C
5%-8C	858.2	VO-8C
5%-4C	862.2	VO-4C
10%-16C	1755.3	VO-16C
10%-12C	1763.3	VO-12C
10%-8C	1772.1	VO-8C
10%-4C	1777.1	VO-4C
15%-16C	2712.0	VO-16C
15%-12C	2715.6	VO-12C
15%-8C	2731.0	VO-8C
15%-4C	2735.2	VO-4C

MD simulations were performed using the GROMACS (version 5.0.6) package.[47–50] In all simulations, periodic boundary conditions and a time step of 2 fs were used. Long range electrostatics was handled with particle mesh Ewald summation method,[51] while short range non-bonded interactions were calculated with a cutoff distance of 1.4 nm. The SETTLE algorithm was used to constrain all bonds in water molecules and the LINCS algorithm was applied to constrain all bonds of solute molecules. In each simulation, the total potential energy was first minimized by static structure optimization. Then, the solvent molecules were relaxed for 1 ns (300 K, 1 bar) around the solutes whose heavy atoms were restrained with a harmonic potential (coefficient = 1000 kJ/(mol nm^2)). After removing the restraint, an NPT ensemble simulation was performed for 80 ns. Full trajectory was obtained by recording the coordinates every 10 ps.

3. RESULTS

In the last 10 ns of the simulation, a large stable aggregate is observed in each of the 12 systems, along with a few smaller aggregates in some systems. The time evolution of number of molecules in the largest aggregates is shown in Figure S2 (Supporting Information Section S2), which remains the same in the last 10 ns. The radial distribution functions (RDFs) for the center of geometry (COG) separation between PA cores are shown in Figure S3 (Supporting Information Section S3). The RDF curves obtained from averages in different 2 ns time windows overlap with each other, which further supports the stability of the aggregates and the attainment of equilibrium. The number of molecules in the largest aggregate quantifies the size of the largest aggregate and the averaged value over last 10 ns is plotted in Figure 2, where data in pure water (0% salt) is adopted from Jian et al.[21] Depending on the length of the side chain, the size of the largest aggregate shows different trend with the salt concentration. Starting with the VO-16C systems, the largest aggregate in 5% salt solution is of the same size as in pure water (all 24 molecules fully aggregated). With further increase of salt, the size decreases to 15 molecules in 10% solution and increases slightly (to 17 molecules) in 15% solution. The trends in the systems containing VO-12C and VO-8C are similar: the largest aggregate is relatively small in pure water (13 and 10 for VO-12C and VO-8C respectively), while the 24 molecules become fully aggregated in 5% and 10% solution; with increase of salt concentration to 15%, the size of the largest aggregate reduces again (to 23 molecules in 15%-12C and 17 molecules in 15%-8C). In the systems containing VO-4C, the aggregate size is 24 in pure water, decreases to 13 with 5% salt addition, increases to 24 again in 10% solution, and finally decreases to 18 at the highest concentration of salt in 15%-4C.

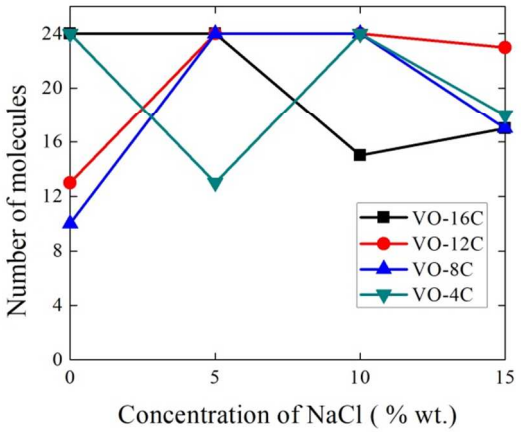

Figure 2. Number of molecules in the largest aggregates plotted against % wt of NaCl in the solution. Data for 0% wt salt (i.e. pure water) were adopted from Jian et al. 2013.[21]

It is clear from the results above that the extent of aggregation can have a non-monotonic dependence on the salt concentration, which differs from the monotonic increasing trend reported by Rezaeidoust et al.[28] The dependence is further sensitive to the molecular structure of the solutes, i.e., the different side chain lengths here. In pure water, the full aggregation of VO-16C molecules was attributed to the mutual association of the long side chains caused by hydrophobic interactions, whereas with the short side chains the full aggregation of VO-4C molecules was due to the stacking of PA cores.[21] The smaller degree of aggregation of VO-8C and VO-12C was caused by the interactions between cores and side chains, which interfered with the core-core stacking.[21] To understand the different trends observed in Figure 2 for different molecules, and whether such difference is caused by different forces driving the aggregation, we quantify the interactions between the model asphaltene molecules via their two regions: the PA core and the side chains.

To do so, each molecule was separated into the two regions, and for any two molecules we calculated: 1) the minimum distance (d_{min}) between the two PA cores, 2) d_{min} between the core region of one molecule and the side chain region of the other molecule, and 3) d_{min} between the two side-chain regions. A π-π contact is said to be formed if d_{min} between the two core regions is ≤ 0.5 nm, a θ−θ contact is recorded if d_{min} between the two side chain regions is ≤ 0.5 nm, and a π−θ contact is said to be present if d_{min} between one core region and one side chain region is ≤ 0.5 nm. The criteria of 0.5 nm was chosen because it corresponds to the distance at which the radial distribution function between the centers of geometry of two PA cores shows the first and most prominent peak in pure water.[21] For a pair of molecules, there can be at most one π−π contact and one θ−θ contact. However, two π−θ contacts can potentially be formed: one between the core of molecule 1 and side chains of molecule 2, and the other between the core of molecule 2 and side chains of molecule 1. Consequently, in any system the maximum possible number of π−θ contacts is twice the maximum possible numbers of π−π and θ−θ contacts. To make a fair comparison, the calculated number of π−θ contacts is divided by two to obtain a scaled value.

Counts of π−π, π−θ (scaled) and θ−θ contacts as functions of time are presented in Figure S4 (Supporting Information, Section S4). In the last 10 ns, the numbers for all 12 systems become stable, and the average values are plotted in Figure 3. As shown in Figure 3a, the number of θ−θ contacts in all 4 systems containing VO-16C is not only 2-3 times the number of π−π contacts, but also much greater than that of π−θ contacts. It is clear that it is the hydrophobic association of the side chains that dominates the aggregation of VO-16C molecules in water. The change of θ−θ contacts with salt concentration also correlates well with the trend of aggregation size shown in Figure 2. Specifically, the number of θ−θ contacts is about the same in pure water and 5% solution, decreases in 10% solution and remains almost the same at 15%. Consistently, Figure 2

also shows the aggregation size at 10% and 15% to be comparable, which is smaller than the aggregates at 0% and 5% (fully aggregated).

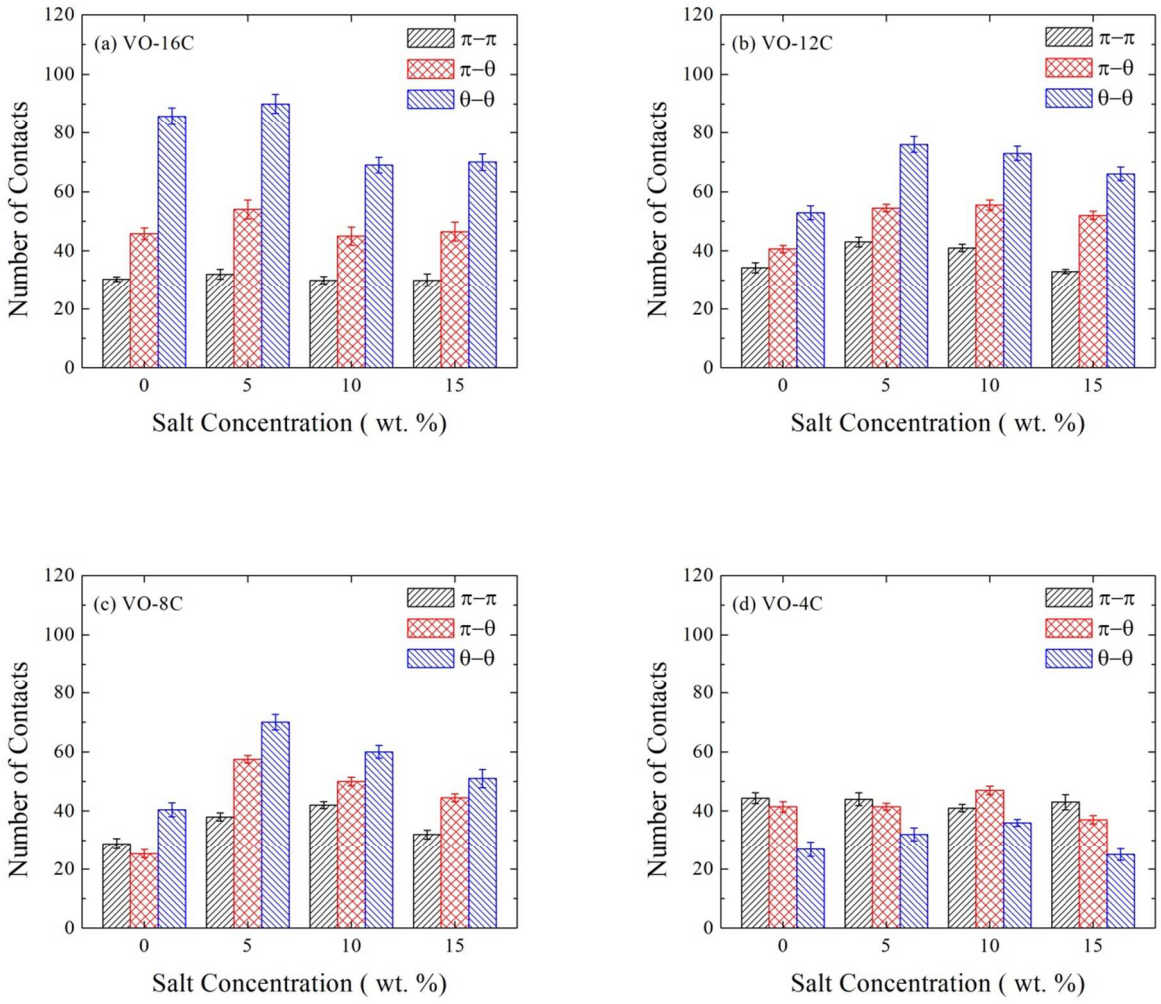

Figure 3. Numbers of π−π, π−θ (scaled) and θ−θ contacts averaged over last 10 ns of simulation for the systems containing: (a) VO-16C, (b) VO-12C, (c) VO-8C, (d) VO-4C. Data for 0% salt are adopted from Jian *et al.* 2013.[21]

Compared with VO-16C, in systems containing VO-12C (Figure 3b), the count of θ−θ contacts have reduced due to the length reduction of the side chains. However, it still appears to be the most important among the three interactions. As the salt concentration increases from 0% to 5%, θ−θ contacts experience a sharp increase; further increase in salt concentration causes it to decrease but very gradually. This again aligns well with results shown in Figure 2, where for systems containing VO-12C, the aggregate increases its size significantly from pure water to 5% solution and becomes fully aggregated, remains fully aggregated at 10% and only decreases slightly at 15%.

Since side chain association plays the most significant role in aggregating VO-16C and VO-12C molecules, the trend observed in Figure 2 for systems containing these two types of molecules can be understood by considering the effect of salt on the aggregation of hydrophobic entities. Zangi *et al.* performed such a study[52] and found that increasing ions with low charge density in a solution promoted the aggregation of hydrophobic particles at low salt concentration but suppressed it at high concentration. Their results were explained by recognizing that the low charge ions behave like co-solutes to the hydrophobic particles at low salt concentration. They increase the aggregation of the hydrophobic particles by withdrawing water from them and adhere to the formed aggregates. When too much salt was introduced, however, the dielectric constant of the solution was significantly decreased, making the hydrophobic particles more soluble in water. The increase of solubility resulted in a reduced tendency for aggregation. That is, there exists a salt concentration at which the salt ions transition from being “co-solute” to being “co-solvent”, and the aggregation of hydrophobic particles is maximized at this transition concentration. Interestingly, the transition concentration was found to depend on the number of

hydrophobic particles in the solution.[52] With more hydrophobic particles, the ions became "co-solvent" at a lower concentration, i.e., the transition concentration is smaller.

If we consider each side chain in the model compounds simulated here as a collection of hydrophobic particles (carbon atoms), the aggregation behaviors observed earlier for VO-16C and VO-12C systems can be explained by the findings of Zangi et al.[52] In the systems containing VO-16C, significant reduction in aggregation (Figure 2) as well as in side chain θ−θ interaction (Figure 3a) occurs after the salt concentration is increased beyond 5%. That is, the transition concentration is around 5% for VO-16C. The side chains in VO-12C are shorter, i.e., the hydrophobic carbon atoms in the systems containing VO-12C are fewer than in those containing VO-16C. It can then be hypothesized that the transition salt concentration may be higher in the VO-12C systems. Indeed, the aggregation size for VO-12C (Figure 2) starts decreasing only after reaching 10%. Although the side chain association (θ−θ contact in Figure 3b) shows signs of decreasing from 5% to 10%, the decrease is very limited and almost negligible if standard deviation in the data is taken into account. More noticeable reduction in the θ−θ contact also occurs after 10%.

While the aggregation of VO-16C and VO-12C is mainly governed by side chain association, and the role of salt can be explained by its effect on the aggregation of carbon atoms, it is not the case for the systems containing VO-8C. If we only considered the aggregation of carbon atoms on the side chains, the smaller number of carbon atoms in VO-8C systems would suggest an even higher transition concentration compared with the VO-12C systems (i.e., at least and possibly beyond 10%). However, in Figure 3c) we see a clear decreasing trend in the number of θ−θ contacts initiated at 5%. In addition, from Figure 3b) to Figure 3c) we see that the number of θ−θ contacts has further decreased and is comparable to the number of π−θ contacts. The above

result implies that the aggregation of VO-8C may also be affected by the interactions involving the core region.

In order to examine the effect of salt addition on the PA cores alone, individual PA cores were created by removing the side chains from the molecules in Figure 1 and MD simulations were carried out on systems containing 6 PA cores in pure water, 5%, 10% and 15% NaCl solutions. The details of the simulations can be found in Supporting Information, Section S5. Each system was simulated for 20 ns, which became stable in the last 3 ns. As shown in Figure 4a, in pure water a 4-molecules aggregate (shown in dashed square) and a dimer are formed, which are separated without mutual interactions. The aggregate has a very ordered structure, with the 4 PA cores stacking to each other in perfect parallel. In 5% solution as shown in Figure 4b, all 6 PA cores form a single aggregate. Five out of the six PA cores are stacked together in parallel fashion while the last one is perpendicular, i.e., forming a T-stacking. When the salt concentration is increased to 10% (Figure 4c), there are one dimer and one 4-molecular aggregate. However, unlike in Figure 4a), only three PA cores in the aggregate form parallel stacking while the other forms a T-stacking (Figure 4C). In 15% solution (Figure 4d), a large aggregate is formed again with 5 molecules in perfect parallel, along with a single dispersed molecule. Clearly the presence of 10% salt has weakened the ability of the PA cores to form parallel stacking. To quantify parallel stacking, the number of direct parallel stacking (DPS) pairs has been calculated. A DPS between two cores is the configuration in which the distance of their geometry centers is within 0.50 nm and the angle between the two cores is near zero (cosine of the angle greater than 0.90).[21] Figure 5 shows the relationship between the number of DPS pairs and salt concentration, where for the core-only systems minimum number of DPS pairs is found in 10% solution.

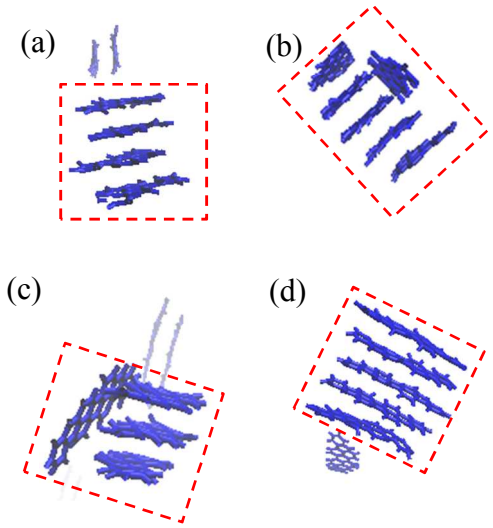

Figure 4. Snapshot of 6 polyaromatic cores in (a) pure water, (b) 5%, (c) 10% and (d) 15% NaCl solutions at the end of 20 ns simulations. Largest aggregates are shown in dashed rectangle.

One possible explanation to this non-monotonic dependence of parallel stacking on salt concentration is the interaction between salt ions and the heteroatoms on the PA cores (Oxygen here). It is well known that the parallel stacking of large aromatic moieties is driven by the interaction between positive σ-framework and negative π-electron cloud.[20] The presence of heteroatoms withdraws the π-electron clouds to reduce the π-π electron repulsion, further enhancing the parallel stacking.[53] When salt ions are introduced, they can establish interactions with the heteroatoms. Our analysis on the distribution of Na^+ ions around the model compounds in Figure S6 (Supporting Information, Section S6) in fact shows that they interact with the oxygen atoms on the PA cores at short distance while having little interaction with the oxygen atoms in the side chains. The attraction between Na^+ ions and oxygen atoms on the cores can reduce the stacking-enhancing effect of the oxygen atoms and negatively impact parallel stacking of the PA cores. The results in Figure 4 seem to suggest that this influence of the salt is little at 5%

salt, but becomes noticeable at 10%. With more salt added (15%), the negative impact of salt is diminished again, possibly due to the strong screening of the electric field under such a high concentration, which has reduced the π-π electron repulsion.

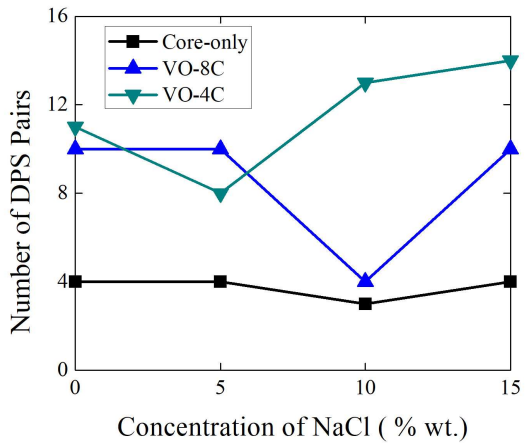

Figure 5. Number of direct parallel stacking pairs for the core-only systems and systems containing VO-8C and VO-4C.

Through the above analysis, it has been demonstrated that the addition of salt can promote aggregation by increasing side chain association (up to a “”co-solute” to “co-solvent” transition concentration); meanwhile it can reduce aggregation by decreasing parallel stacking of the cores for intermediate concentration. In the systems containing VO-8C, the number of DPS pairs shows the same trend as the core-only systems (Figure 5). Although the effect of salt on hydrophobic association of side chains, if isolated, would have predicted higher intermolecular interactions at 10% than at 5%, the reduced capability of forming parallel stacking at 10% has led to the decrease in the numbers of π−θ and θ−θ contacts as the salt concentration changes from 5% to 10% (Figure 3c). The results also indicate that there are mutual influences of the

core-core, chain-chain and core-chain interactions in VO-8C, because the length of side chains is comparable to the size of the PA core.

Interestingly, the reduced parallel stacking at 10% did not cause the overall π−π contacts to decrease. Instead, the number of π−π contacts in Figure 3c increases as the salt concentration changes from 5% to 10%. The reason for this seemingly contradictory observation is that while the capability of forming parallel stacking is weaker at 10%, T-stacking between cores increases (see Figure 4). T-stacking is able to compensate for the loss of parallel stacking, which leads to the same aggregation size at 10% as the size at 5% (Figure 2). However, the aggregate structures are less compact with T-stacking (as shown in Supporting Information Section S7). T-stacking also limits the core-chain and chain-chain interactions at 10%, as shown in Figure 3c.

Finally, in VO-4C systems (Figure 3d), the side chains are so short that the θ−θ interaction becomes the smallest among the three. The aggregation through hydrophobic interaction becomes less dominant. On the other hand, despite the short side chains, the aggregation of VO-4C molecules is not entirely controlled by core-core interaction. In fact, the trend of aggregation size shown in Figure 2 is not the same as that of π−π contacts in Figure 3d. The counting of DPS pairs shows that the smallest number of DPS pairs occurs at 5%, as shown in Figure 5. This is different from the VO-8C systems, as well as the systems without side chains (Figure 5); in both cases the DPS is weakest at 10%. Given that the side chains in VO-4C are the shortest; its behaviors would have been expected to be closest to the model without side chains. The counterintuitive results we observed suggest that the role of the rather short side chains in VO-4C is not negligible in the presence of salt, although the exact mechanism still remains inconclusive and to be further explored. Nevertheless, the smallest DPS at 5% does agree with the smallest aggregation size at 5% for VO-4C (Figure 2), even though the number of π−π

contacts (Figure 3d) is not reduced at 5%. T-stacking in this case appears to be incapable of compensating for the loss of DPS, as it did for the VO-8C systems. As for the decreased aggregation size again at 15% (Figure 2), it is similar to the cases of VO-12C and VO-8C and is caused by the significant reduction in of π−θ and θ−θ interactions from 10% to 15% (Figure 3d)), possibly due to the transition of salt from "co-solute" to "co-solvent".

4. Discussion

It is worth commenting on our results in comparison to two experimental works that studied the effect of salt on asphaltene accumulation on oil/water interface. Verruto et al. [54] observed that the salt addition delayed the formation and consolidation of asphaltene film at heptol/water interface. Chávez-Miyauchi et al.[55] reported a non-monotonic relationship between the elasticity of asphaltene film on crude oil/water interface and salt concentration. Both works attributed the effect of salt to the screening of electrostatic interactions between asphaltenes. Compared with these studies, the electrostatic interaction in our work is expected to be weaker. Firstly, the model compounds simulated in this work (based on VO-78) are likely to be less polar than real asphaltenes used in the experiments. As shown in Figure S1, the model compounds have partial charges at the oxygen atoms and their neighboring carbon atoms, while the rest of the molecules carry zero or negligible partial charges. Furthermore, the two studies considered oil/water interface, which can be negatively charged and provide a strong electrostatic driving force. Such an interface is absent in our systems. As a result, the electrostatic interaction in our work is weaker and is manifested via the core-core interaction. The added salt interacts with the heteroatoms (oxygen) on the cores, which in turn affects the core-core interaction.

On the other hand, in bulk water the hydrophobic association of side chains provides another mechanism for the aggregation. Rankin et al.[56] studied the interaction between small hydrocarbon groups (CH_3OH and $C_4H_{10}O$) in water, and reported the contact between them to be random rather than hydrophobic. In our work, however, the hydrophobic moieties are much larger. Even VO-4C, with shortest side chain length, contains 5 hydrocarbon groups on each side chain. There is strong evidence of association of side chains, as shown by the stable θ−θ contacts found in the last stage of simulation (Figure S4). Studying modified VO-78 with different side chain lengths has allowed us to address the role of side chain association, and their joint effect with the electrostatic interaction among the cores. There has been a large body of simulation work [57–61] that has provided fundamental understanding of interaction between hydrophobic entities, including quantification of the interaction between two hydrophobic solutes using the potential of mean force (PMF). Similar PMF calculation for our model compounds is of interest, but performing constraint MD simulations to obtain the PMF is out of the scope of this work.

Asphaltenes are known to absorb onto oil/water interface and stabilized the oil-in-water or water-in-oil emulsion. Many researchers have reported the accumulation of asphaltene at the oil/water interface in the form of aggregates.[54,55] Molecular arrangement in the aggregates can affect the rheological properties of the asphaltene films, thereby influencing the emulsion stability. The presence of salt can affect the interfacial adsorption of asphaltenes via two ways. Firstly, it can change the amount of asphaltenes accumulation on the interface. For instance, the MD simulation performed by Jian et al.[62] reported that salt addition increased the accumulation of asphaltene onto toluene/water interface. Secondly, the presence of salt can affect the interaction among asphaltene aggregates, thus affect the structure of asphaltene film.[54,55] The model compound (VO-79) simulated by Jian et al.[62] has a similar structure to VO-8C studied in the

present work. Our results have shown that the aggregate size of VO-8C has non-monotonic dependence on salt concentration, reaching a maximum at intermediate concentration. One could then hypothesize that intermediate salt concentration might be most detrimental in terms of stabilizing the emulsion, since it will lead to not only large amount of adsorption, but also large aggregates that form a rigid film. Confirming this hypothesis, however, would require a series of simulations with different salt concentration applied to a water/oil/asphaltene system.

5. CONCLUSIONS

Using molecular dynamics simulations, we studied the aggregations of 4 types of asphaltene model compounds, VO-16C, VO-12C, VO-8C and VO-4C, in aqueous solution with different NaCl concentrations. Our results, for the first time, revealed complex non-monotonic relationship between the aggregation size and salt concentration. In addition, the four compounds, having the same polyaromatic core but different side chain length, exhibited different dependence on salt addition. Hydrophobic association between side chains are the predominant driving force for aggregation in systems containing VO-16C and VO-12C molecules which have longer side chain length. The change of aggregation size with salt concentration is positively correlated to the effect of salt on hydrophobic interaction: it promotes the hydrophobic interaction at low concentration but suppresses it at high concentration. In systems with VO-8C molecules, which have intermediate side chain length, the aggregation is not only dependent on the hydrophobic association between chains, but also influenced by core-core and core-side chain interactions. In systems containing VO-4C with shortest side chain, while salt addition has a significant effect on the core-core interaction, the short side chains still play a non-negligible role in aggregation with the presence of salt.

ACKNOWLEDGMENTS

The authors acknowledge the computing resources and technical support from Western Canada Research Grid (WestGrid). The authors also gratefully acknowledge the financial support from the Natural Science and Engineering Research Council of Canada (NSERC) and the Future Energy Systems under the Canada First Research Excellence Fund.

Supporting Information. Partial charges and charge groups, evolution of number of molecules in largest aggregates, radial distribution function for center of geometry of PA cores, evolution of interactions, detailed information on simulation of polyaromatic cores, radial distribution function of Na^+ around atoms, and snapshot.

REFERENCES

(1) Speight, J. G. Petroleum Asphaltenes - Part 1: Asphaltenes, Resins and the Structure of Petroleum. *Oil Gas Sci. Technol.* **2004**, *59* (5), 467–477.

(2) Fortuny, M.; Oliveira, C. B. Z.; Melo, R. L. F. V.; Nele, M.; Coutinho, R. C. C.; Santos, A. F. Effect of Salinity, Temperature, Water Content, and PH on the Microwave Demulsification of Crude Oil Emulsions †. *Energy & Fuels* **2007**, *21* (3), 1358–1364.

(3) Borges, B.; Rondón, M.; Sereno, O.; Asuaje, J. Breaking of Water-in-Crude-Oil Emulsions. 3. Influence of Salinity and Water−Oil Ratio on Demulsifier Action. *Energy & Fuels* **2009**, *23* (3), 1568–1574.

(4) Byambajav, E.; Ohtsuka, Y. Cracking Behavior of Asphaltene in the Presence of Iron Catalysts Supported on Mesoporous Molecular Sieve with Different Pore Diameters. *Fuel* **2003**, *82* (13), 1571–1577.

(5) Zekri, A. Y.; Shedid, S. A. The Effect of Fracture Characteristics on Reduction of Permeability by Asphaltene Precipitation in Carbonate Formation. *J. Pet. Sci. Eng.* **2004**, *42* (2–4), 171–182.

(6) Rahmani, N. H. G.; Dabros, T.; Masliyah, J. H. Evolution of Asphaltene Floc Size Distribution in Organic Solvents under Shear. *Chem. Eng. Sci.* **2004**, *59* (3), 685–697.

(7) Sayyad Amin, J.; Nikooee, E.; Ayatollahi, S.; Alamdari, A. Investigating Wettability Alteration Due to Asphaltene Precipitation: Imprints in Surface Multifractal Characteristics. *Appl. Surf. Sci.* **2010**, *256* (21), 6466–6472.

(8) Mclean, J. D.; Kilpatrick, P. K. Effects of Asphaltene Solvency on Stability of Water-in-Crude-Oil Emulsions. *J. Colloid Interface Sci.* **1997**, *189* (189), 242–253.

(9) Nenningsland, A. L.; Gao, B.; Simon, S.; Sjöblom, J. Comparative Study of Stabilizing

Agents for Water-in-Oil Emulsions. *Energy and Fuels* **2011**, *25* (12), 5746–5754.

(10) Zhang, L.; Shi, C.; Lu, Q.; Liu, Q.; Zeng, H. Probing Molecular Interactions of Asphaltenes in Heptol Using a Surface Forces Apparatus: Implications on Stability of Water-in-Oil Emulsions. *Langmuir* **2016**, *32* (19), 4886–4895.

(11) Shi, C.; Zhang, L.; Xie, L.; Lu, X.; Liu, Q.; Mantilla, C. A.; Van Den Berg, F. G. A.; Zeng, H. Interaction Mechanism of Oil-in-Water Emulsions with Asphaltenes Determined Using Droplet Probe AFM. *Langmuir* **2016**, *32* (10), 2302–2310.

(12) Jian, C.; Liu, Q.; Zeng, H.; Tang, T. Effect of Model Polycyclic Aromatic Compounds on the Coalescence of Water-in-Oil Emulsion Droplets. *J. Phys. Chem. C* **2017**, *121* (19), 10382–10391.

(13) Barré, L.; Jestin, J.; Morisset, A.; Palermo, T.; Simon, S. Relation between Nanoscale Structure of Asphaltene Aggregates and Their Macroscopic Solution Properties. *Oil Gas Sci. Technol. – Rev. IFP* **2009**, *64* (5), 617–628.

(14) Mullins, O. C.; Sabbah, H.; Eyssautier, J.; Pomerantz, A. E.; Barré, L.; Andrews, a. B.; Ruiz-Morales, Y.; Mostowfi, F.; McFarlane, R.; Goual, L.; et al. Advances in Asphaltene Science and the Yen–Mullins Model. *Energy & Fuels* **2012**, *26* (7), 3986–4003.

(15) Mullins, O. C. The Modified Yen Model †. *Energy & Fuels* **2010**, *24* (4), 2179–2207.

(16) Schuler, B.; Meyer, G.; Peña, D.; Mullins, O. C.; Gross, L. Unraveling the Molecular Structures of Asphaltenes by Atomic Force Microscopy. *J. Am. Chem. Soc.* **2015**, *137* (31), 9870–9876.

(17) Groenzin, H.; Mullins, O. C. Asphaltene Molecular Size and Structure. *J. Phys. Chem. A* **1999**, *103* (50), 11237–11245.

(18) Groenzin, H.; Mullins, O. C. Molecular Size and Structure of Asphaltenes from Various

Sources. *Energy* **2000**, No. 12, 677–684.

(19) Eyssautier, J.; Levitz, P.; Espinat, D.; Jestin, J.; Gummel, J.; Grillo, I.; Barré, L. Insight into Asphaltene Nanoaggregate Structure Inferred by Small Angle Neutron and X-Ray Scattering. *J. Phys. Chem. B* **2011**, *115* (21), 6827–6837.

(20) Hunter, C. A.; Sanders, J. K. M. The Nature of .Pi.-.Pi. Interactions. *J. Am. Chem. Soc.* **1990**, *112* (14), 5525–5534.

(21) Jian, C.; Tang, T.; Bhattacharjee, S. Probing the Effect of Side-Chain Length on the Aggregation of a Model Asphaltene Using Molecular Dynamics Simulations. *Energy & Fuels* **2013**, *27* (4), 2057–2067.

(22) Jian, C.; Tang, T.; Bhattacharjee, S. Molecular Dynamics Investigation on the Aggregation of Violanthrone78-Based Model Asphaltenes in Toluene. *Energy & Fuels* **2014**, *28* (6), 3604–3613.

(23) Lashkarbolooki, M.; Ayatollahi, S.; Riazi, M. Effect of Salinity, Resin, and Asphaltene on the Surface Properties of Acidic Crude Oil/Smart Water/Rock System. *Energy & Fuels* **2014**, *28* (11), 6820–6829.

(24) Hezave, A. Z.; Dorostkar, S.; Ayatollahi, S.; Nabipour, M.; Hemmateenejad, B. Investigating the Effect of Ionic Liquid (1-Dodecyl-3-Methylimidazolium Chloride ([C12mim] [Cl])) on the Water/Oil Interfacial Tension as a Novel Surfactant. *Colloids Surfaces A Physicochem. Eng. Asp.* **2013**, *421*, 63–71.

(25) Sheng, J. J. Critical Review of Low-Salinity Waterflooding. *J. Pet. Sci. Eng.* **2014**, *120*, 216–224.

(26) Shariatpanahi, S. F.; Strand, S.; Austad, T. Initial Wetting Properties of Carbonate Oil Reservoirs: Effect of the Temperature and Presence of Sulfate in Formation Water.

Energy and Fuels **2011**, *25* (7), 3021–3028.

(27) Lashkarbolooki, M.; Ayatollahi, S. Effect of Asphaltene and Resin on Interfacial Tension of Acidic Crude Oil/ Sulfate Aqueous Solution: Experimental Study. *Fluid Phase Equilib.* **2016**, *414*, 149–155.

(28) Rezaeidoust, A.; Puntervold, T.; Strand, S.; Austad, T. Smart Water as Wettability Modifier in Carbonate and Sandstone: A Discussion of Similarities/Differences in the Chemical Mechanisms. *Energy and Fuels* **2009**, *23* (9), 4479–4485.

(29) Chaala, A.; Benallal, B.; Hachelef, S. Investigation on the Flocculation of Asphaltenes and the Colloidal Stability of the Crude Oil Fraction. *Can. J. Chem. Eng.* **1994**, *72* (6), 1036–1041.

(30) Liu, J.; Zhang, L.; Xu, Z.; Masliyah, J. Colloidal Interactions between Asphaltene Surfaces in Aqueous Solutions. *Langmuir* **2006**, *22* (4), 1485–1492.

(31) Zhang, L.; Xie, L.; Shi, C.; Huang, J.; Liu, Q.; Zeng, H. Mechanistic Understanding of Asphaltene Surface Interactions in Aqueous Media. *Energy & Fuels* **2017**, *31* (4), 3348–3357.

(32) Mikami, Y.; Liang, Y.; Matsuoka, T.; Boek, E. S. Molecular Dynamics Simulations of Asphaltenes at the Oil–Water Interface: From Nanoaggregation to Thin-Film Formation. *Energy & Fuels* **2013**, *27* (4), 1838–1845.

(33) Lashkarbolooki, M.; Riazi, M.; Ayatollahi, S.; Zeinolabedini Hezave, A. Synergy Effects of Ions, Resin, and Asphaltene on Interfacial Tension of Acidic Crude Oil and Low-High Salinity Brines. *Fuel* **2016**, *165*, 75–85.

(34) Moeini, F.; Hemmati-Sarapardeh, A.; Ghazanfari, M. H.; Masihi, M.; Ayatollahi, S. Toward Mechanistic Understanding of Heavy Crude Oil/Brine Interfacial Tension: The

Roles of Salinity, Temperature and Pressure. *Fluid Phase Equilib.* **2014**, *375*, 191–200.

(35) Sakthivel, S.; Velusamy, S.; Nair, V. C.; Sharma, T.; Sangwai, J. S. Interfacial Tension of Crude Oil-Water System with Imidazolium and Lactam-Based Ionic Liquids and Their Evaluation for Enhanced Oil Recovery under High Saline Environment. *Fuel* **2017**, *191*, 239–250.

(36) Andrews, A. B.; McClelland, A.; Korkeila, O.; Demidov, A.; Krummel, A.; Mullins, O. C.; Chen, Z. Molecular Orientation of Asphaltenes and PAH Model Compounds in Langmuir−Blodgett Films Using Sum Frequency Generation Spectroscopy. *Langmuir* **2011**, *27* (10), 6049–6058.

(37) Manuel F. González; Clementina Sosa Stull; Francisco López-Linares, A.; Pereira-Almao*, P. Comparing Asphaltene Adsorption with Model Heavy Molecules over Macroporous Solid Surfaces. *Energy & Fuels* **2007**, *21* (1), 234–241.

(38) Jarne, C.; Cebolla, V. L.; Membrado, L.; Le Mapihan, K.; Giusti, P. High-Performance Thin-Layer Chromatography Using Automated Multiple Development for the Separation of Heavy Petroleum Products According to Their Number of Aromatic Rings. *Energy & Fuels* **2011**, *25* (10), 4586–4594.

(39) Jian, C.; Tang, T. Molecular Dynamics Simulations Reveal Inhomogeneity-Enhanced Stacking of Violanthrone-78-Based Polyaromatic Compounds in n-Heptane-Toluene Mixtures. *J. Phys. Chem. B* **2015**, *119* (27), 8660–8668.

(40) Jian, C.; Tang, T. One-Dimensional Self-Assembly of Polyaromatic Compounds Revealed by Molecular Dynamics Simulations. *J. Phys. Chem. B* **2014**, *118* (44), 12772–12780.

(41) Schüttelkopf, A. W.; van Aalten, D. M. F.; IUCr. *PRODRG* : A Tool for High-Throughput Crystallography of Protein–ligand Complexes. *Acta Crystallogr. Sect. D Biol. Crystallogr.*

2004, *60* (8), 1355–1363.

(42) Oostenbrink, C.; Villa, A.; Mark, A. E.; Van Gunsteren, W. F. A Biomolecular Force Field Based on the Free Enthalpy of Hydration and Solvation: The GROMOS Force-Field Parameter Sets 53A5 and 53A6. *J. Comput. Chem.* **2004**, *25* (13), 1656–1676.

(43) Jian, C.; Tang, T.; Bhattacharjee, S. A Dimension Map for Molecular Aggregates. *J. Mol. Graph. Model.* **2015**, *58*, 10–15.

(44) Kuznicki, T.; Masliyah, J. H.; Bhattacharjee, S. Molecular Dynamics Study of Model Molecules Resembling Asphaltene-Like Structures in Aqueous Organic Solvent Systems. *Energy & Fuels* **2008**, *22* (4), 2379–2389.

(45) Kuznicki, T.; Masliyah, J. H.; Bhattacharjee, S. Aggregation and Partitioning of Model Asphaltenes at Toluene−Water Interfaces: Molecular Dynamics Simulations. *Energy & Fuels* **2009**, *23* (10), 5027–5035.

(46) Zhu, X.; Chen, D.; Wu, G. Molecular Dynamic Simulation of Asphaltene Co-Aggregation with Humic Acid during Oil Spill. *Chemosphere* **2015**, *138*, 412–421.

(47) Hess, B. P-LINCS: A Parallel Linear Constraint Solver for Molecular Simulation. *J. Chem. Theory Comput.* **2008**, *4* (1), 116–122.

(48) Van Der Spoel, D.; Lindahl, E.; Hess, B.; Groenhof, G.; Mark, A. E.; Berendsen, H. J. C. GROMACS: Fast, Flexible, and Free. *J. Comput. Chem.* **2005**, *26* (16), 1701–1718.

(49) Lindahl, E.; Hess, B.; van der Spoel, D. GROMACS 3.0: A Package for Molecular Simulation and Trajectory Analysis. *J. Mol. Model.* **2001**, *7* (8), 306–317.

(50) Berendsen, H. J. C.; van der Spoel, D.; van Drunen, R. GROMACS: A Message-Passing Parallel Molecular Dynamics Implementation. *Comput. Phys. Commun.* **1995**, *91* (1–3), 43–56.

(51) Essmann, U.; Perera, L.; Berkowitz, M. L.; Darden, T.; Lee, H.; Pedersen, L. G. A Smooth Particle Mesh Ewald Method. *J. Chem. Phys.* **1995**, *103* (19), 8577–8593.

(52) Zangi, R.; Berne, B. J. Aggregation and Dispersion of Small Hydrophobic Particles in Aqueous Electrolyte Solutions. *J. Phys. Chem. B* **2006**, *110* (45), 22736–22741.

(53) Sedghi, M.; Goual, L.; Welch, W.; Kubelka, J. Effect of Asphaltene Structure on Association and Aggregation Using Molecular Dynamics. *J. Phys. Chem. B* **2013**, *117* (18), 5765–5776.

(54) Verruto, V. J.; Le, R. K.; Kilpatrick, P. K. Adsorption and Molecular Rearrangement of Amphoteric Species at Oil-Water Interfaces. *J. Phys. Chem. B* **2009**, *113* (42), 13788–13799.

(55) Chávez-Miyauchi, T. E.; Firoozabadi, A.; Fuller, G. G. Nonmonotonic Elasticity of the Crude Oil-Brine Interface in Relation to Improved Oil Recovery. *Langmuir* **2016**, *32* (9), 2192–2198.

(56) Rankin, B. M.; Ben-Amotz, D.; Van Der Post, S. T.; Bakker, H. J. Contacts between Alcohols in Water Are Random Rather than Hydrophobic. *J. Phys. Chem. Lett.* **2015**, *6* (4), 688–692.

(57) Choudhury, N. On the Manifestation of Hydrophobicity at the Nanoscale. *J. Phys. Chem. B* **2008**, *112* (20), 6296–6300.

(58) Choudhury, N.; Pettitt, B. M. On the Mechanism of Hydrophobic Association of Nanoscopic Solutes. *J. Am. Chem. Soc.* **2005**, *127* (10), 3556–3567.

(59) Choudhury, N.; Pettitt, B. M. The Dewetting Transition and the Hydrophobic Effect. *J. Am. Chem. Soc.* **2007**, *129* (15), 4847–4852.

(60) Wallqvist, A.; Berne, B. J. Molecular Dynamics Study of the Dependence of Water

Solvation Free Energy on Solute Curvature and Surface Area. *J. Phys. Chem* **1995**, *99*, 2885–2892.

(61) Huang, X.; Margulis, C. J.; Berne, B. J. Dewetting-Induced Collapse of Hydrophobic Particles. *Proc. Natl. Acad. Sci.* **2003**, *100* (21), 11953–11958.

(62) Jian, C.; Poopari, M. R.; Liu, Q.; Zerpa, N.; Zeng, H.; Tang, T. Mechanistic Understanding of the Effect of Temperature and Salinity on the Water/Toluene Interfacial Tension. *Energy & Fuels* **2016**, *30* (12), 10228–10235.